

# Synthesis, anti-tuberculosis activity, and 3D-QSAR study of 4-(adamantan-1-yl)-2-substituted quinolines

Amit Nayyar,<sup>a,†</sup> Vikramdeep Monga,<sup>a</sup> Alpeshkumar Malde,<sup>b</sup>  
Evans Coutinho<sup>b,\*</sup> and Rahul Jain<sup>a,\*</sup>

<sup>a</sup>Department of Medicinal Chemistry, National Institute of Pharmaceutical Education and Research,  
Sector 67, S.A.S. Nagar, Punjab 160 062, India

<sup>b</sup>Department of Pharmaceutical Chemistry, Bombay College of Pharmacy, Kalina, Santacruz (E), Mumbai 400 098, India

Received 5 September 2006; accepted 30 October 2006  
Available online 1 November 2006

**Abstract**—Structural optimization of the previously identified 4-(adamantan-1-yl)-2-quinolinecarbohydrazide (AQCH, MIC = 6.25 µg/mL, 99% inhibition, *Mycobacterium tuberculosis* H37Rv) has led to two series of 4-(adamantan-1-yl)-2-substituted quinolines (Series 1–2). All new derivatives were evaluated in vitro for antimycobacterial activities against drug-sensitive *M. tuberculosis* H37Rv strain. Several 4-adamantan-1-yl-quinoline-2-carboxylic acid *N'*-alkylhydrazides (Series 1) described herein showed promising inhibitory activity. In particular, analogs **7**, **9**, **20**, and **21** displayed MIC of 3.125 µg/mL. Further investigation of AQCH by its reaction with various aliphatic, aromatic, and heteroaromatic aldehydes led to the synthesis of 4-adamantan-1-yl-quinoline-2-carboxylic acid alkylidene hydrazides (Series 2). Analogs **42–44** and **48** have produced promising antimycobacterial activities (99% inhibition) at 3.125 µg/mL against drug-sensitive *M. tuberculosis* H37Rv strain. The most potent analog **35** of the series produced 99% inhibition at 1.00 µg/mL against drug-sensitive strain, and MIC of 3.125 µg/mL against isoniazid-resistant TB strain. To understand the relationship between structure and activity, a 3D-QSAR analysis has been carried out by three methods—comparative molecular field analysis (CoMFA), CoMFA with inclusion of a hydrophathy field (HINT), and comparative molecular similarity indices analysis (CoMSIA). Several statistically significant CoMFA, CoMFA with HINT, and CoMSIA models were generated. Prediction of the activity of a test set of molecules was the best for the CoMFA model generated with database alignment. Based on the CoMFA contours, we have tried to explain the structure–activity relationships of the compounds reported herein.

© 2006 Elsevier Ltd. All rights reserved.

## 1. Introduction

Tuberculosis (TB) is a treatable contagious disease and despite availability of useful drugs continues to kill approximately 2 million people worldwide each year.<sup>1</sup> The factors responsible for this are: (i) patient non-compliance to existing drug regimens which has resulted in the emergence of single drug-resistant strains to all major anti-TB drugs; (ii) emergence of multidrug-resistant TB (MDR-TB), which is defined as the disease caused by the strains of *Mycobacterium tuberculosis* resistant to two mainstay first-line anti-TB drugs, isoniazid and

rifampicin; and (iii) association of human immunodeficiency virus (HIV) with TB, in which TB is the leading cause of death among patients who are HIV-positive.<sup>2</sup> Consequently, new drugs with divergent and unique structure and with a mechanism of action possibly different from that of existing drugs are urgently required.

Recently, a broad structure-based bio-evaluation of several new chemical entities against various pathogens including *M. tuberculosis* led us to identify ring-substituted quinolines as a new structural class of anti-TB agents.<sup>3</sup> The ring-substituted quinolines inhibit both drug-sensitive and drug-resistant *M. tuberculosis* in vitro. The structural optimization of ring-substituted quinolines to maximize anti-TB activity resulted in several promising analogs.<sup>4–8</sup> Of note, two analogs, 2,8-dicyclopropyl-4-methylquinoline (**1**, DCMQ)<sup>3</sup> and 4-(adamantan-1-yl)-2-quinolinecarbohydrazide (**2**, AQCH)<sup>6</sup> (Fig. 1), displayed promising activities against

**Keywords:** Tuberculosis; Ring-substituted quinolines; Synthesis; 3D-QSAR study; COMFA; COMSIA; HINT.

\* Corresponding authors. Tel.: +91 22 26670871; fax: +91 22 26670816 (E.C.), tel.: +91 172 2214682; fax: +91 172 2214692 (R.J.); e-mail addresses: [evans@bcpindia.org](mailto:evans@bcpindia.org); [rahuljain@niper.ac.in](mailto:rahuljain@niper.ac.in)

† Present address: Astrazeneca India Pvt. Ltd, R&D, Bangalore, India.

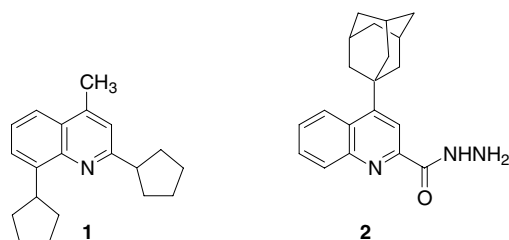


Figure 1. Structures of promising ring-substituted quinolines.

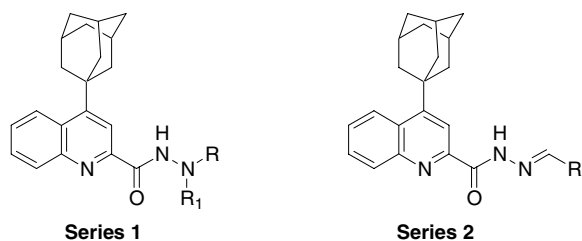


Figure 2. General structure of the synthesized ring-substituted quinolines.

drug-sensitive and drug-resistant *M. tuberculosis* H37Rv strains and were considered important lead molecules. The lack of cross-resistance with currently used anti-TB agents suggests that ring-substituted quinolines possibly act on a novel, yet unknown target. This observation is supported by the fact that ring-substituted quinolines **1** and **2** did not inhibit *M. tuberculosis* purified DNA gyrase, the target for quinolones (unpublished data). The short (1–3 overall steps), facile, and inexpensive synthesis of ring-substituted quinolines is considered another important factor which made us to embark on further structural optimization of this class. We report herein the synthesis and anti-TB activity of two new series of 4-adamantan-1-yl group containing 2-substituted quinolines (Series 1–2, Fig. 2) that is a direct outcome of our efforts to optimize **2**. As remarked earlier, the potential TB drug-target(s) for the ring-substituted quinolines remains unknown. As a result, we have also used the ligand-based approach of 3D-QSAR by CoMFA, CoMFA in conjunction with HINT, a hydrophobic field evaluator, and CoMSIA for understanding the SAR of the synthesized compounds.

## 2. Chemistry

Commercially available quinoline-2-carboxylic acid (**3**) was easily converted to its ethyl ester hydrochloride derivative by reaction with abs ethyl alcohol and passing a slow stream of dry HCl gas through the reaction solution. The hydrochloride salt upon neutralization with 25% NH<sub>4</sub>OH afforded ethyl 2-quinolinecarboxylate (**4**). The key step of the synthesis involved the regioselective alkylation at the C-4 position of the quinoline ring. This was accomplished by a direct homolytic free radical alkylation reaction of **4** via a silver-catalyzed oxidative decarboxylation of 1-adamantanecarboxylic acid by ammonium persulfate in the presence of 10% sulfuric

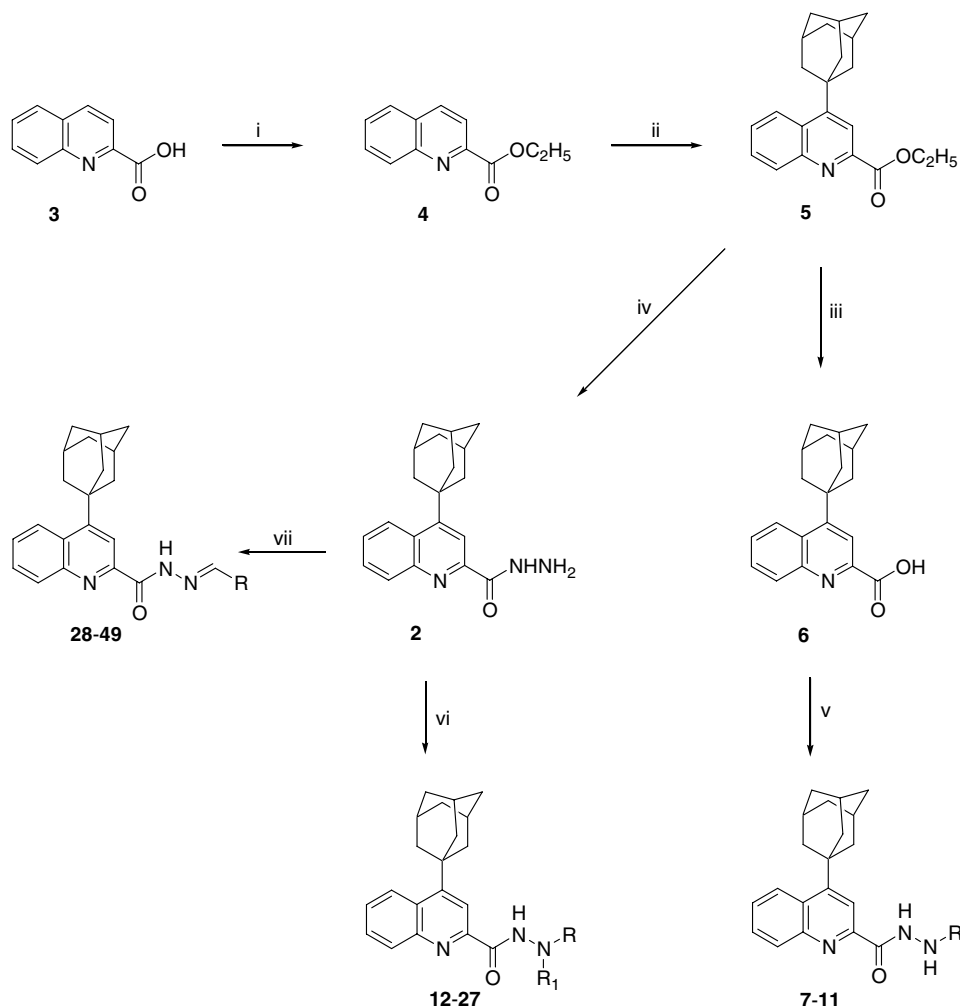
acid and CH<sub>3</sub>CN as solvent to produce ethyl 4-(adamantan-1-yl)-2-quinolinecarboxylate (**5**). The reaction proceeded through a homolytic free radical mechanism, and offered a unique procedure of functionalization of the electron-deficient quinoline ring with alkyl groups of various sizes.<sup>9,10</sup> Ethyl 4-(adamantan-1-yl)-2-quinolinecarboxylate (**5**) upon acidic hydrolysis with 6 N HCl at reflux temperature gave 4-(adamantan-1-yl)-2-quinolinecarboxylic acid hydrochloride (**6**). The latter compound **6** was then treated with thionyl chloride in anhydrous dichloroethane (DCE) at 80 °C for 2 h to provide corresponding acid chloride, which upon reaction in situ with various substituted hydrazines in anhydrous dichloromethane (DCM) in the presence of triethylamine (Et<sub>3</sub>N) at 4 °C for 1 h afforded 4-adamantan-1-yl-quinoline-2-carboxylic acid *N'*-alkylhydrazides **7–11** (Scheme 1).

Ethyl 4-(adamantan-1-yl)-2-quinolinecarboxylate (**5**) was conveniently and quantitatively converted to 4-(adamantan-1-yl)-2-quinolinecarbohydrazide (**2**) by reaction with hydrazine hydrate in 95% ethyl alcohol at 80 °C for 8 h.<sup>6</sup> Primary alkyl halides were successfully treated with **2** in the presence of Et<sub>3</sub>N in abs ethyl alcohol at 80 °C for 8 h to produce an easily separable mixture of 4-adamantan-1-yl-quinoline-2-carboxylic acid *N'*-alkylhydrazides and 4-adamantan-1-yl-quinoline-2-carboxylic acid *N,N'*-dialkylhydrazides **12–19** and **23–27**. However, reaction of **2** with secondary alkyl halides in the presence of Et<sub>3</sub>N using conditions used for primary alkyl halides did not offer desired product. Alternatively, replacement of Et<sub>3</sub>N with K<sub>2</sub>CO<sub>3</sub> in the presence of *N,N*-dimethylformamide (DMF) as a solvent at 80 °C for 8 h successfully reacted **2** with secondary alkyl halides to produce adamantan-1-yl-quinoline-2-carboxylic acid *N'*-alkylhydrazides **20–22** (Scheme 1).

Finally, 4-(adamantan-1-yl)-2-quinolinecarbohydrazide **2** upon reaction with various commercially available aliphatic, aromatic, and heteroaromatic aldehydes in the presence of abs ethyl alcohol at 80 °C for 2 h easily produced 4-adamantan-1-yl-quinoline-2-carboxylic acid alkylidene hydrazides **28–49** (Scheme 1).

## 3. Biological activity

In vitro activities of the synthesized derivatives (Series 1–4) against *M. tuberculosis* H37Rv strain (ATCC 27294, susceptible both to rifampicin and isoniazid) were initially carried out using the microplate alamar blue assay (MABA) at a concentration of 6.25 µg/mL.<sup>11</sup> Compounds exhibiting fluorescence were then tested in the BACTEC 460 radiometric system<sup>12</sup> and the % inhibition data are summarized in Tables 1 and 2. Compounds demonstrating ≥90% inhibition at 6.25 µg/mL in the primary screen were also tested at the lower concentration of 3.125 and 1.0 µg/mL to determine MIC value that is defined as the minimum concentration exhibiting 99% inhibition. Isoniazid (99% inhibition, MIC = 1 µg/mL) was included, as a standard drug, for comparison.



**Scheme 1.** Reagents and conditions: (i) abs EtOH, HCl gas, 4 °C, 2 h, 25% NH<sub>4</sub>OH solution; (ii) AgNO<sub>3</sub>, 1-adamantanecarboxylic acid, (NH<sub>4</sub>)<sub>2</sub>S<sub>2</sub>O<sub>8</sub>, CH<sub>3</sub>CN, 10% H<sub>2</sub>SO<sub>4</sub>, 70–80 °C, 15 min; (iii) 6 N HCl, 100 °C, 8 h; (iv) NH<sub>2</sub>NH<sub>2</sub>·H<sub>2</sub>O, 95% EtOH, 80 °C, 8 h; (v) SOCl<sub>2</sub>, DCE, 80 °C, 2 h; RNHNH<sub>2</sub>, Et<sub>3</sub>N, DCM, 4 °C, 1 h; (vi) RX, Et<sub>3</sub>N, abs EtOH, 80 °C, 8 h or RBr, K<sub>2</sub>CO<sub>3</sub>, DMF, 80 °C, 8 h; (vii) RCHO, abs EtOH, 80 °C, 2 h.

Analogues **10** (R = C<sub>6</sub>H<sub>4</sub>-*o*-F, R<sub>1</sub> = H), **11** (R = C<sub>6</sub>H<sub>4</sub>-*p*-F, R<sub>1</sub> = H) and **16** (R = CH(CH<sub>3</sub>)C<sub>2</sub>H<sub>5</sub>, R<sub>1</sub> = H) exhibited promising activity and inhibited the growth of mycobacteria to 99%, 93%, and 97%, respectively, at the test concentration of 6.25 µg/mL. Analogues **7** (R = COCH<sub>3</sub>, R<sub>1</sub> = H), **20** (R = *c*-C<sub>5</sub>H<sub>9</sub>, R<sub>1</sub> = H) and **21** (R = *c*-C<sub>6</sub>H<sub>11</sub>, R<sub>1</sub> = H) were most active of the series and inhibited the growth of drug-sensitive *M. tuberculosis* H37Rv by 99% at the lower test dose of 3.125 µg/mL. The remaining analogs of the Series 1 produced modest inhibition in the range of 19–82% at 6.25 µg/mL (Table 1). In agreement with our earlier observation, fluorophenyl group containing analogs have shown promising anti-TB activity.<sup>8</sup> A general observation of the SAR indicates that 4-adamantan-1-yl-quinoline-2-carboxylic acid *N'*-alkylhydrazides produce superior anti-TB activity compared to 4-adamantan-1-yl-quinoline-2-carboxylic acid *N'*,*N'*-dialkylhydrazides.

Analogues **28–49** (Series 2) exhibited modest to promising anti-TB activity (Table 2). For example, analogs **32** (R = C<sub>6</sub>H<sub>4</sub>-*m*-OH) and **49** (R = 7-chloroquinolin-4-yl) exhibited 99% and 95% inhibition of drug-sensitive *M. tuberculosis* H37Rv, respectively, at 6.25 µg/mL. While,

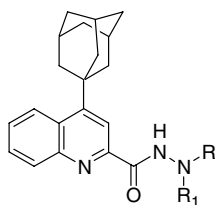
analogues **42** (R = 1*H*-pyrrol-2-yl), **43** (R = thiophen-2-yl), **44** (R = furan-2-yl), and **48** (R = quinolin-4-yl) produced 99% inhibition at a lower test dose of 3.125 µg/mL. The most potent analogue **35** (R = C<sub>6</sub>H<sub>4</sub>-*o*-Cl) of the series exhibited 99% inhibition at the lowest tested dose of 1.00 µg/mL and was comparable to standard isoniazid. The remaining analogs of the series exhibited inhibition ranged between 10% and 84% against *M. tuberculosis* H37Rv at 6.25 µg/mL.

The most active derivative, 4-adamantan-1-yl-quinoline-2-carboxylic acid (2-chlorobenzylidene)hydrazide (**35**), was also evaluated for antimycobacterial activity against isoniazid-resistant strain of *M. tuberculosis* H37Rv and exhibited promising activity (99% inhibition, MIC = 3.125 µg/mL).

## 4. Computational details

### 4.1. Dataset

The set of 44 molecules (Tables 1 and 2) was used in the 3D-QSAR study. The dataset was divided into a

**Table 1.** In vitro antimycobacterial activity and pIC<sub>50</sub>s of 4-adamantan-1-yl-quinoline-2-carboxylic acid *N'*-alkylhydrazides and *N',N'*-dialkylhydrazides **7–27** (Series 1) against drug-sensitive *M. tuberculosis* H37Rv strain

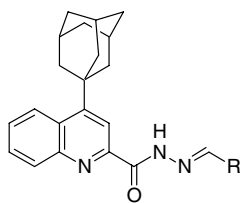
Compound	R	R <sub>1</sub>	Test concn (μg/mL)	% inhibition	pIC <sub>50</sub>
<b>2</b>	H	H	6.250	99	6.71
<b>7</b>	COCH <sub>3</sub>	H	3.125	99	7.06
<b>8</b>	CHO	H	6.250	19	4.12
<b>9</b>		H	3.125	99	7.12
<b>10</b>		H	6.250	99	6.82
<b>11</b>		H	6.250	93	5.95
<b>12</b>	(CH <sub>2</sub> ) <sub>2</sub> CH <sub>3</sub>	H	6.250	82	5.42
<b>13</b>	(CH <sub>2</sub> ) <sub>2</sub> CH <sub>3</sub>	(CH <sub>2</sub> ) <sub>2</sub> CH <sub>3</sub>	6.250	75	5.29
<b>14</b>	(CH <sub>2</sub> ) <sub>3</sub> CH <sub>3</sub>	H	6.250	55	4.87
<b>15</b>	(CH <sub>2</sub> ) <sub>3</sub> CH <sub>3</sub>	(CH <sub>2</sub> ) <sub>3</sub> CH <sub>3</sub>	6.250	64	5.09
<b>16</b>	CH(CH <sub>3</sub> )C <sub>2</sub> H <sub>5</sub>	H	6.250	97	6.29
<b>17</b>	(CH <sub>2</sub> ) <sub>5</sub> CH <sub>3</sub>	H	6.250	77	5.32
<b>18</b>	(CH <sub>2</sub> ) <sub>5</sub> CH <sub>3</sub>	(CH <sub>2</sub> ) <sub>5</sub> CH <sub>3</sub>	6.250	65	5.14
<b>19</b>	CH <sub>2</sub> CH=CH <sub>2</sub>	CH <sub>2</sub> CH=CH <sub>2</sub>	6.250	22	4.26
<b>20</b>	<i>c</i> -C <sub>5</sub> H <sub>9</sub>	H	3.125	99	7.09
<b>21</b>	<i>c</i> -C <sub>6</sub> H <sub>11</sub>	H	3.125	99	7.11
<b>22</b>	CH(CH <sub>3</sub> ) <sub>2</sub>	H	6.250	51	4.78
<b>23</b>		H	6.250	65	5.10
<b>24</b>			6.250	55	5.02
<b>25</b>		H	6.250	50	4.85
<b>26</b>			6.250	45	4.86
<b>27</b>			6.250	51	4.95

training set (30 molecules) and a test set (14 molecules: id's **7, 8, 9, 11, 16, 20, 21, 25, 37, 36, 45, 46, 48, and 49**) by means of chemical as well as biological diversity. Daylight fingerprints of the molecules along with the pIC<sub>50</sub> data were used to separate the molecules into training and test sets based on the Tanimoto similarity coefficient.<sup>13</sup>

#### 4.2. Biological data

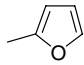
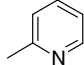
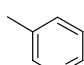
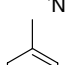
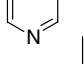
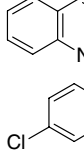
For the QSAR study, the activity values were transformed as follows<sup>14</sup>

$$\text{Activity} = -\log c + \log t$$

**Table 2.** In vitro antimycobacterial activity and pIC<sub>50</sub>s of 4-adamantan-1-yl-quinoline-2-carboxylic acid alkylidene hydrazides **28–49** (Series 2) against drug-sensitive *M. tuberculosis* H37Rv strain

Compound	R	Test concn (µg/mL)	% inhibition	pIC <sub>50</sub>
<b>28</b>	CH <sub>2</sub> CH <sub>3</sub>	6.250	69	5.11
<b>29</b>	CH(CH <sub>3</sub> ) <sub>2</sub>	6.250	63	5.01
<b>30</b>	C(CH <sub>3</sub> ) <sub>3</sub>	6.250	10	3.84
<b>31</b>		3.125	99	7.11
<b>32</b>		6.250	99	6.83
<b>33</b>		6.250	73	5.27
<b>34</b>		6.250	20	4.25
<b>35</b>		1.000	99	7.64
<b>36</b>		6.250	16	4.18
<b>37</b>		6.250	64	5.19
<b>38</b>		6.250	69	5.24
<b>39</b>		6.250	57	5.02
<b>40</b>		6.250	79	5.48
<b>41</b>		6.250	66	5.2
<b>42</b>		3.125	99	7.10
<b>43</b>		3.125	99	7.12

Table 2 (continued)

Compound	R	Test concn ( $\mu\text{g/mL}$ )	% inhibition	$\text{pIC}_{50}$
44		3.125	99	7.10
45		6.250	84	5.54
46		6.250	53	4.87
47		6.25	70	5.19
48		3.125	99	7.16
49		6.25	95	6.18

where  $c$  is molar concentration = concentration ( $\mu\text{g/mL}$ ) \* 0.001/(molecular weight)

$$\text{logit} = \log[\% \text{ inhibition}/(100 - \% \text{ inhibition})].$$

#### 4.3. Molecular modeling

The CoMFA,<sup>15</sup> CoMSIA<sup>16</sup>, and CoMFA with HINT<sup>17</sup> studies were carried out using SYBYL 7.1<sup>18</sup> installed on a Pentium 2.8 GHz PC with the Linux OS (Red Hat Enterprise WS 3.0). The 4-(adamantan-1-yl)quinoline is a rigid moiety. At the C2-position of the quinoline ring, three basic moieties –CONHNHCO–, –CONHNRR<sub>1</sub>, and –CONHN=CHR are present. The geometries of these groups were derived from the crystal structures—**sg6059** (for molecules 7 and 8), **cf6244** (for molecules 2 and 9–27), and **bt2126** (for molecules 28–49) (Fig. 3).<sup>19</sup>

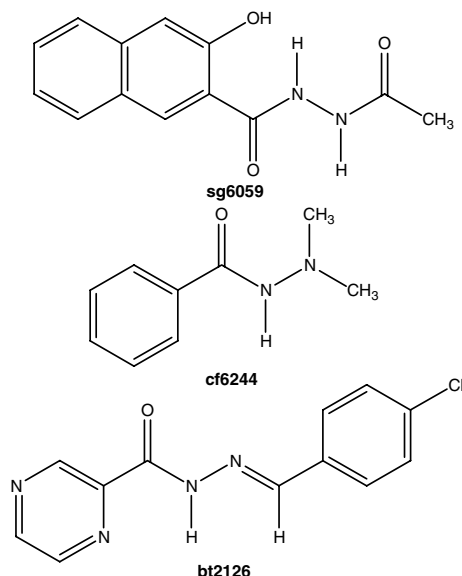


Figure 3. Structures of the reported molecules whose X-ray data were used for building the molecules.

The structures of the molecules were built with the *Sketcher* module and energy minimized by Powell's method using the MMFF94<sup>20</sup> force field with a distance-dependent dielectric term. The geometries of the R and R<sub>1</sub> groups were optimized by subjecting the molecules to molecular dynamics (MD) simulation keeping the remaining part of the structure fixed. This was accomplished by heating to 700 K for 1 ps and slowly annealing to 200 K in steps of 100 K for 1 ps at each temperature, with a step size of 1 fs; and snapshots were captured every 5 fs. The lowest energy structure from the MD trajectory was sent through a final round of minimization. The minimization was terminated at a maximum value of 0.5 kcal/mol/Å for the gradient.

#### 4.4. Alignment

The most crucial input for the *CoMFA* is the alignment of the molecules. Molecule 35 with the highest activity and the least conformational flexibility was chosen as the template and all other molecules were aligned to it using the database alignment method in SYBYL (Fig. 4). The molecules were aligned with reference to the quinoline ring. A second alignment was also carried out using the *FIELD FIT* method, wherein the steric and electrostatic fields around the molecules were superimposed over the same fields of the template molecule.

#### 4.5. CoMFA interaction energy calculation

The steric and electrostatic fields in CoMFA were calculated at each lattice intersection of a regularly spaced grid of 2.0 Å in all three dimensions within the defined region. A sp<sup>3</sup> carbon atom with +1.0 charge was used as the probe. The van der Waals potential and Coulombic energy between the probe and the molecule were calculated using the standard Tripos force field. A distance-dependent dielectric constant of 1.0 $r$  was used in the calculation of the electrostatics. The steric field was truncated at points where the value exceeded +/30.0 kcal/mol,



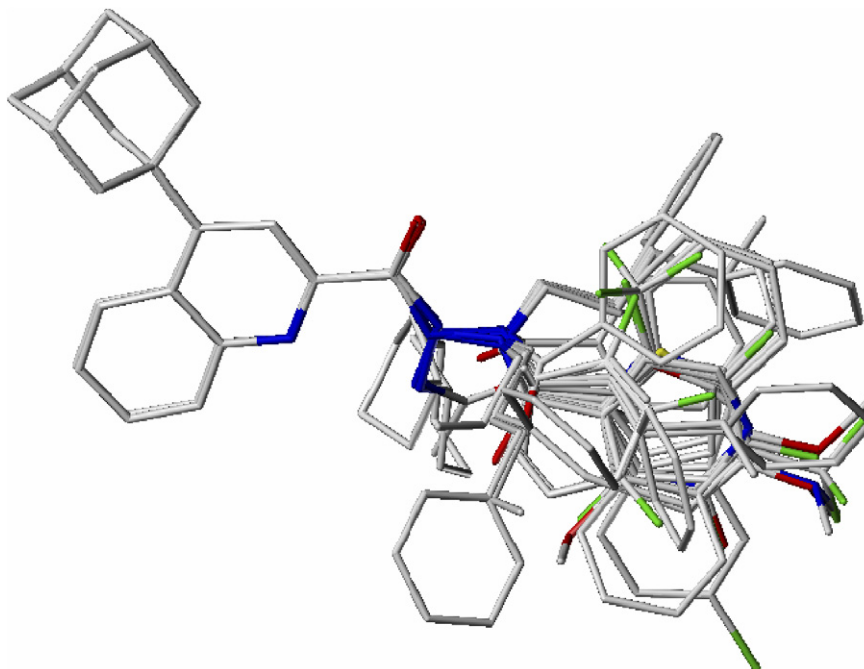


**Figure 4.** A view of the molecules aligned using database alignment.

and the electrostatic fields were ignored at those lattice points where the steric interactions were high.

#### 4.6. HINT hydropathic field calculation

The hydropathic fields were calculated with the *HINT* module in *SYBYL*. The region defined for calculation of the CoMFA fields was also used to describe the space in which the *HINT* fields were generated. *HINT* calculates the hydrophobic interaction between all atom pairs in a molecule using the following equation

$$B = \sum \sum b_{ij}$$

where,  $b_{ij}$ ,  $a_i a_j S_i S_j R_{ij} T_{ij}$

$b_{ij}$ , micro-interaction constant representing the attraction/interaction between atoms  $i$  and  $j$

$a_i$ , the hydrophobic atom constant for atom  $i$

$S_i$ , the solvent accessible surface area for atom  $i$

$R_{ij}$ , the functional distance behavior for the interaction between atoms  $i$  and  $j$

$T_{ij}$ , a discriminant function designed to keep the signs of interactions consistent with the *HINT* convention that favorable interactions are positive and unfavorable interactions are negative.

#### 4.7. CoMSIA interaction energy calculations

Five CoMSIA fields—steric, electrostatic, hydrophobic, and hydrogen-bond donor and acceptor potentials were calculated at each lattice intersection of a regularly

spaced grid of 2.0 Å. A probe atom with radius 1.0 Å, +1.0 charge, hydrophobicity of +1.0, and hydrogen-bond donor and acceptor properties of +1.0 was used to calculate steric, electrostatic, hydrophobic, and hydrogen-bond donor and acceptor fields. The contribution from each one of these descriptors was truncated above 0.3 kcal/mol.

#### 4.8. Partial least squares (PLS) analysis

The PLS method was used to set up a correlation between the molecular fields and the inhibitory activity of the molecules. The optimal number of components was determined with *SAMPLS*<sup>21</sup> (Samples-distance partial least square) and cross-validation was carried out by the *leave-one-out* method. The model with the optimum number of components (highest  $q^2$ ) and with the lowest standard error of prediction (SDEP) was considered for further analysis. Equal weights were assigned to the steric and electrostatic fields by the *COMFA\_STD* scaling option. To speed up the analysis and reduce noise, columns with a  $\sigma$  value below 2.0 kcal/mol were filtered off. Final analysis was performed to calculate the conventional  $r^2$  using the optimum number of components. To further assess the robustness and statistical confidence of the derived models, bootstrapping<sup>22</sup> analysis for 10 runs was performed. Bootstrapping involves the generation of many new datasets from the original dataset and is obtained by randomly choosing samples from the original dataset. The statistical calculation is performed on each of these bootstrap samplings. The difference between the parameters calculated from the original dataset and the average of the parameters calculated from the many bootstrap samplings is a measure of the bias of the original calculations. Models with a cross-validation ( $q^2$ ) value above 0.3 were sought, since

at this value the probability of chance correlation is less than 5%.<sup>23</sup>

#### 4.9. Predictive correlation coefficient

The predictive ability of each 3D-QSAR model was determined from a set of 24 test molecules not included in the model generation. The predictive correlation coefficient ( $r^2_{\text{pred}}$ ), based on the test set molecules, is defined as

$$r^2_{\text{pred}} = (\text{SD} - \text{PRESS})/\text{SD}$$

where SD is the sum of squared deviations between the biological activity of the test set and the mean activity of the training set molecules and the PRESS is the sum of squared deviations between predicted and actual activity values for every molecule in the test set.

#### 4.10. CoMFA contour maps

Contour maps were generated as a scalar product of coefficients and standard deviation (StDev \* Coeff) associated with each column. Favored and disfavored levels, fixed at 80% and 20%, respectively, were used to display the steric and the electrostatic fields. The contours for steric fields are shown in green (more bulk favored) and yellow (less bulk favored), while the electrostatic field contours are displayed in red (electronegative substituents favored) and blue (electropositive substituents favored) colors.

#### 4.11. Results and discussion

The geometry of the groups at the 2-position of the quinoline ring was adopted from the X-ray structures of related molecules. The variation in biological activity is approximately four log units. The CoMFA and CoMSIA models were generated for both the alignments, namely database and field fit. The hydrophobic field calculated using *HINT* was used in conjunction with CoMFA fields to derive additional models. The statistics of

the models generated are shown in Table 3. The activity of molecule **8** in the test set was poorly predicted (+2.0 U) by all six models. Hence, this molecule was considered as an outlier and not included in the calculation of the predictive correlation coefficient ( $r^2_{\text{pred}}$ ).

The CoMFA models obtained by both the alignments (Models 1 and 4) and only the CoMSIA model (with steric, electrostatic, and hydrophobic fields, Model 3) obtained by database alignment exhibit the best statistics for the training set and test sets. Among the three, Model 1, that is, CoMFA model obtained by database alignment, has overall the best statistical qualities, a cross-validated correlation coefficient ( $q^2$ ) of 0.60, conventional correlation coefficient ( $r^2$ ) of 0.94, and predictive correlation coefficient ( $r^2_{\text{pred}}$ ) of 0.49. A plot of the predicted versus experimental activity for the training set molecules using Model 1 is shown in Figure 5. The incorporation of the hydrophobic field of *HINT* to the CoMFA models does not improve the statistical quality of the models. The statistical data in Table 3 indicate that the steric and electrostatic fields are sufficient to generate a 3D-QSAR model with good correlation and predictive power.

The CoMFA model, with its hundreds or thousands of terms, is generally represented as a 3D ‘coefficient contour.’ Colored contours in the map represent those areas in 3D space where changes in the steric and electrostatic field values of a compound correlate strongly with concomitant change in its biological activity. The CoMFA steric and electrostatic contour plots of Model 1 are shown in Figures 6 and 7, respectively, and these are seen clustered around the groups R, R' present at the hydrazone nitrogen.

Analysis of steric contours (Fig. 6) reveals two green colored contours and one small yellow colored contour. One green contour lies in the plane of the quinoline ring near the phenyl ring in molecule **35**, while the other one lies outside the plane of the phenyl ring. The bulkier

**Table 3.** A summary of the statistics of the 3D-QSAR models

Parameter	Database alignment			Field fit alignment		
	CoMFA Model 1	CoMFA + HINT Model 2	CoMSIA (SEH) Model 3	CoMFA Model 4	CoMFA + HINT Model 5	CoMSIA (SEH) Model 6
<i>N</i>	5	5	6	6	6	6
$r^2$	0.94	0.95	0.96	0.96	0.96	0.96
$r^2_{\text{cv}}$	0.60	0.46	0.48	0.54	0.49	0.42
<i>SEE</i>	0.25	0.24	0.22	0.20	0.20	0.23
<i>F</i> -value	100.1	88.5	84.9	103.5	100.4	80.6
$r^2_{\text{pred}}$	0.49	0.23	0.43	0.43	0.33	0.34
$r^2_{\text{bs}}$	0.94	0.94	0.96	0.97	0.95	0.96
SD	0.03	0.04	0.01	0.02	0.03	0.02
Contributions (%)						
Steric	56	46	17	54	42	17
Electrostatic	44	38	53	46	40	53
Hydrophobic	—	16	30	—	18	30

$r^2_{\text{cv}}$ , cross-validated correlation coefficient using *SAMPLS*; *N*, optimum number of components;  $r^2$ , conventional (non cross-validated) correlation coefficient; *SEE*, standard error of estimate;  $r^2_{\text{pred}}$ , predictive (test molecules) correlation coefficient;  $r^2_{\text{bs}}$ , correlation coefficient after 10 runs of bootstrapping analysis; SD, standard deviation from 10 bootstrapping runs.



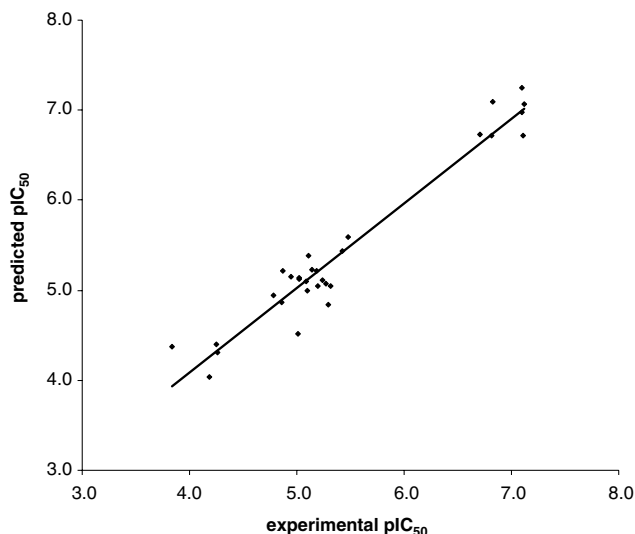


**Figure 5.** Predicted versus experimental activity for molecules in the training set based on Model 1.

substituents like the phenyl ring in molecules **9**, **10**, **11**, **31**, **32**, and **35** and the quinoline ring in **48** and **49**, attached to the hydrazone moiety, are buried partly in the green contour present in the plane of the quinoline ring. All these molecules exhibit good activity. In molecules **12–18** and **23–26**, one of the alkyl substituents attached to hydrazone nitrogen is partially buried in the other green contour outside the plane of the quinoline ring. As a result, these molecules exhibit moderate activity. Among these, molecule **16**, with the *sec*-butyl

substituent, exhibits the highest activity. It has a branched alkyl substituent, with a greater portion buried in the sterically favorable green contours, while other similar molecules with an unbranched alkyl substituent only partially fill the favorable region, and hence have much lower activities. Molecules **20** and **21** also exhibit good activity and contain the cycloalkyl substituent. This indicates that the bulky branched chain and cycloalkyl substituents are favored on the hydrazone nitrogen as well as the phenyl and quinoline substituents are favored on hydrazone nitrogen.

Analysis of the electrostatic contours (Fig. 4) shows three red colored contours and one blue colored contour. The two red colored contours lie perpendicular to one face of phenyl ring in **35**, while the third one lies on the opposite face. The blue contour lies near the phenyl ring in the plane of the quinoline ring. The N, S, O, and Cl atoms of the pyrrole (**42**), thiophene (**43**), furan (**44**), and phenyl (**35**) rings, respectively, lie near these red colored contours. The electronegative substituents are at the favored positions in these molecules and hence, these molecules exhibit good activity. Likewise, the hydroxyl group in **32**, the oxygen atom of the acetyl group in **7**, and the nitrogen atom of *o*-pyridyl group in **45** lie near the electrostatically favorable red contours, and consequently these molecules exhibit good activity. The dimethylamino substituent in **40** is buried completely in the blue colored contour which is favored for methyl groups but disfavored for nitrogen, and as a result, **40** has moderate activity. In molecule **37**, the *o*-CF<sub>3</sub> group lies near the favored red contour, while the second *p*-CF<sub>3</sub> group is

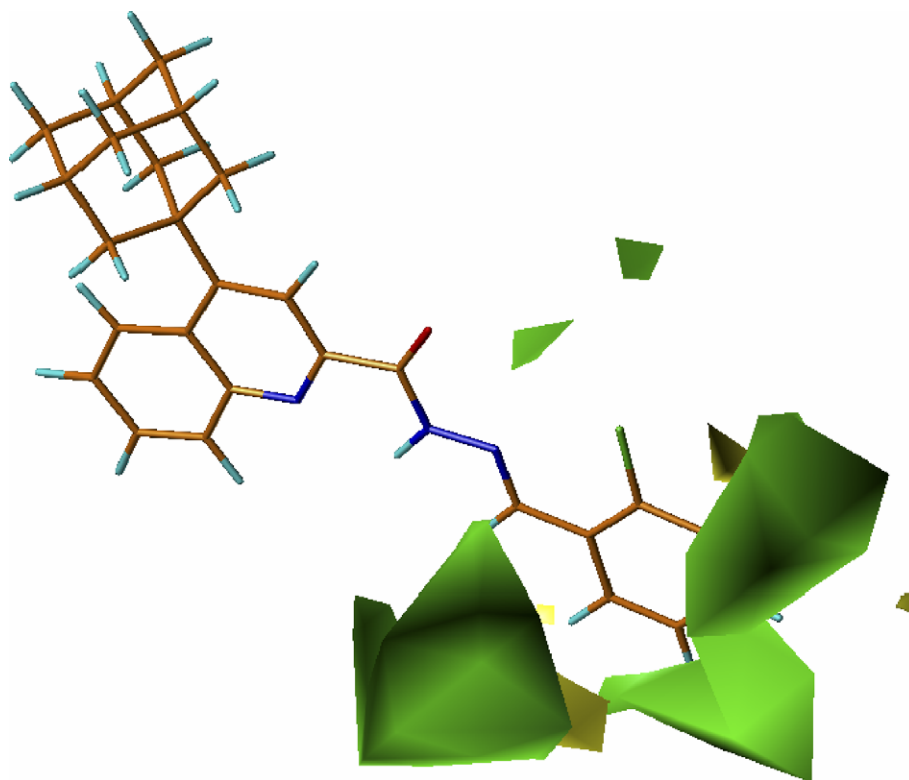


**Figure 6.** A map of the CoMFA contour (Model 1) for steric fields drawn around molecule **35**. The green colored contour favors steric bulk, while sites where steric bulk is disfavored are shown in yellow.

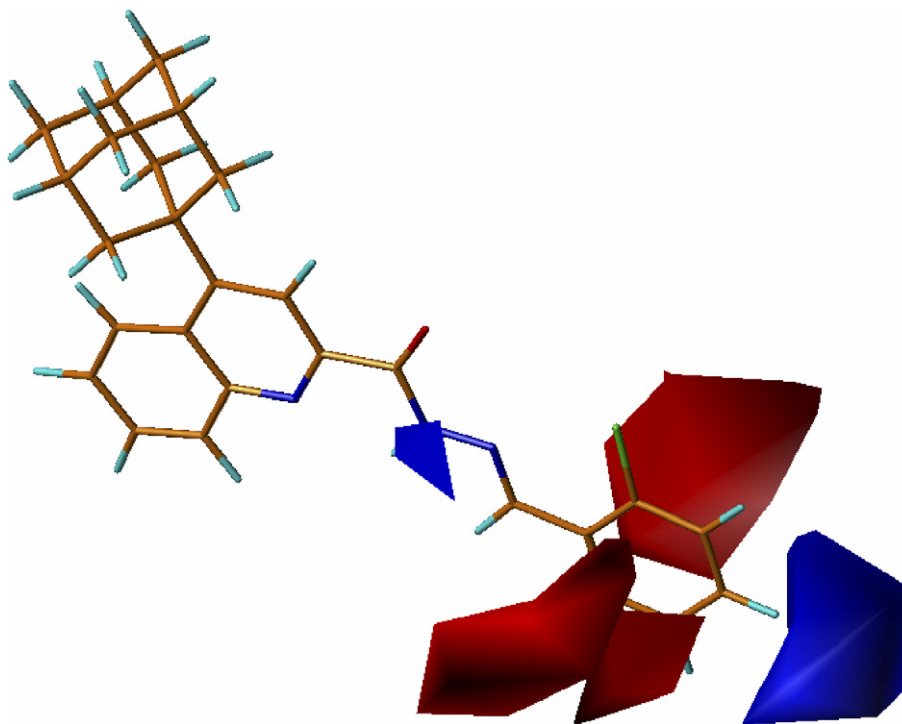


**Figure 7.** CoMFA contour map (Model 1) for electrostatic fields drawn around molecule **35**. The red contour shows regions where electronegative substituents are favored, while the blue contour is associated with positions where electropositive substituents improve activity.

buried in the unfavorable blue contour, and consequently, it exhibits moderate activity.

## 5. Conclusions

In our efforts to optimize previously identified lead 4-(adamantan-1-yl)-2-quinolinecarbohydrazide **2**, we synthesized two new series of 2-substituted quinolines containing 4-(adamantan-1-yl) group. Analogs **7**, **9**, **20**, and **21** of the 4-(adamantan-1-yl)-quinoline-2-carboxylic acid *N'*-alkylhydrazides (Series 1) exhibited promising anti-TB activity (99% inhibition) at 3.125 µg/mL. While four analogs **42–44** and **48** of the 4-(adamantan-1-yl)-quinoline-2-carboxylic acid alkylidene/arylidene/heteroarylidene hydrazides (Series 2) produced 99% inhibition at 3.125 µg/mL. The most potent compound 4-(adamantan-1-yl)-quinoline-2-carboxylic acid (2-chlorobenzylidene)hydrazide (**35**) inhibited drug-sensitive *M. tuberculosis* H37Rv at 1.00 µg/mL (99% inhibition) and was equipotent to standard drug isoniazid. Thus, ring-substituted quinolines reported herein may be considered attractive for further optimization to obtain compounds with greater potency. To understand structure–activity relationship of the reported compounds, a 3D-QSAR analysis was carried out using CoMFA alone, CoMFA in conjunction with a hydrophobic field evaluated using HINT, and CoMSIA, to map the structural features contributing to the inhibitory activity of these molecules. Inclusion of the HINT hydrophobic field to the CoMFA models does not improve the quality of the models. The CoMSIA models are comparable in most aspects to the CoMFA models but lack good predictive power. The database alignment of molecules produced models with better statistics than those with

field fit alignment. Out of the various models evaluated, the CoMFA model based on database alignment produced a statistically sound model with a good correlation and predictive power. Analysis of the CoMFA contours provides details on the fine relationship linking structure and activity, and offers clues for structural modifications that can improve the activity.

## 6. Experimental

Melting points were recorded on a Mettler DSC 851 instrument or a capillary melting point apparatus and are uncorrected. <sup>1</sup>H spectra were recorded on a 300 MHz Bruker FT-NMR (Avance DPX300) spectrometer using tetramethylsilane as internal standard and the chemical shifts are reported in δ units. Mass spectra were recorded on a HRMS (Finnigan Mat LCQ) spectrometer using ESI mode. Elemental analyses were carried out on an Elementar Vario EL spectrometer. Chromatographic purifications were carried out with silica gel 60 (230–400 mesh) and TLC (silica gel) was done on silica gel coated (Merck Kiesel 60 F<sub>254</sub>, 0.2 mm thickness) sheets. All chemicals were purchased from Aldrich Chemical Ltd (Milwaukee, WI, USA). Solvents used for the chemical synthesis were acquired from commercial sources, were of analytical grade and used without further purification unless otherwise stated.

### 6.1. Synthesis of 4-(adamantan-1-yl)-2-quinolinecarboxylic acid·HCl (**6**)

A solution of ethyl 4-(adamantan-1-yl)-2-quinolinecarboxylate<sup>6</sup> (**5**, 2 g, 10 mmol) in 6 N HCl (20 mL) was heated

at 100 °C for 8 h. 4-(Adamantan-1-yl)-2-quinolinecarboxylic acid hydrochloride (**6**) was obtained directly by evaporation of the acid hydrolysis solution. Yield: 95%; mp: 124–126 °C; <sup>1</sup>H NMR (CD<sub>3</sub>OD): δ 8.47 (d, 1H, *J* = 8.5 Hz), 7.95 (d, 1H, *J* = 7.1 Hz), 7.77 (s, 1H), 7.54 (m, 1H), 7.44 (m, 1H), 1.88 (m, 15H); ESIMS: *m/z* 308 (M+1); Anal. Calcd for C<sub>20</sub>H<sub>22</sub>ClNO<sub>2</sub> (343.8): C, 69.86; H, 6.45; N, 4.07. Found: C, 69.92; H, 6.63; N, 4.32.

## 6.2. General procedure for synthesis of 4-adamantan-1-yl-quinoline-2-carboxylic acid *N'*-alkylhydrazides (7–11)

To a mixture of 4-(adamantan-1-yl)-2-quinolinecarboxylic acid hydrochloride (**6**, 0.1 g, 0.3 mmol) in anhydrous DCE (10 mL), SOCl<sub>2</sub> (60 μL, 0.9 mmol) was added. Reaction mixture was heated at 80 °C for 2 h. Excess of reagents were removed under reduced pressure to afford acid chloride intermediate in situ. This intermediate was dissolved in anhydrous DCM (15 mL) and allowed to react with various aliphatic or aromatic hydrazides in the presence of triethylamine (100 μL, 0.7 mmol) at 4 °C for 1 h. Reaction mixture was diluted with DCM (25 mL), washed with water (2 × 15 mL), brine solution (15 mL), and dried over Na<sub>2</sub>SO<sub>4</sub>. The organic layer was concentrated under reduced pressure to afford crude product which was purified by flash column chromatography on silica gel using EtOAc/hexanes (7:93) as eluant to provide 4-adamantan-1-yl-quinoline-2-carboxylic acid *N'*-alkylhydrazides **7–11**.

**6.2.1. 4-Adamantan-1-yl-quinoline-2-carboxylic acid *N'*-acetylhydrazide (**7**).** Yield: 37%; mp: 212–214 °C (dec); IR (KBr): 3219, 1638 cm<sup>-1</sup>; <sup>1</sup>H NMR (CDCl<sub>3</sub>): δ 10.40 (br s, 1H), 8.65 (d, 1H, *J* = 9.0 Hz), 8.16 (m, 2H), 7.70 (m, 1H), 7.58 (m, 1H), 1.88 (m, 15H), 1.25 (s, 3H); ESIMS: *m/z* 364 (M+1); Anal. Calcd for C<sub>22</sub>H<sub>25</sub>N<sub>3</sub>O<sub>2</sub> (363.1): C, 72.70; H, 6.93; N, 11.56. Found: C, 72.78; H, 6.97; N, 11.60.

**6.2.2. 4-Adamantan-1-yl-quinoline-2-carboxylic acid *N'*-formylhydrazide (**8**).** Yield: 20%; mp: 175–177 °C (dec); IR (KBr): 3317, 1650 cm<sup>-1</sup>; <sup>1</sup>H NMR (CDCl<sub>3</sub>): δ 8.81 (s, 1H), 8.67 (d, 1H, *J* = 8.7 Hz), 8.29 (s, 1H), 8.17 (d, 1H, *J* = 6.7 Hz), 7.71 (m, 1H), 7.54 (m, 1H), 1.88 (m, 15H); ESIMS: *m/z* 350 (M+1); Anal. Calcd for C<sub>21</sub>H<sub>23</sub>N<sub>3</sub>O<sub>2</sub> (349.2): C, 72.18; H, 6.63; N, 12.03. Found: C, 72.20; H, 6.67; N, 12.07.

**6.2.3. 4-Adamantan-1-yl-quinoline-2-carboxylic acid *N'*-(2-fluorophenyl)hydrazide (**9**).** Yield: 65%; semi-solid; IR (KBr): 3274, 1678 cm<sup>-1</sup>; <sup>1</sup>H NMR (CDCl<sub>3</sub>): δ 9.79 (br s, 1H), 8.69 (d, 1H, *J* = 8.6 Hz), 8.19 (m, 2H), 7.74 (m, 1H), 7.61 (m, 1H), 7.02 (m, 3H), 6.88 (m, 1H), 1.88 (m, 15H); ESIMS: *m/z* 416 (M+1); Anal. Calcd for C<sub>26</sub>H<sub>26</sub>FN<sub>3</sub>O (415.5): C, 75.16; H, 6.31; N, 10.11. Found: C, 75.8; H, 6.25; N, 10.05.

**6.2.4. 4-Adamantan-1-yl-quinoline-2-carboxylic acid *N'*-(3-fluorophenyl)hydrazide (**10**).** Yield: 60%; semi-solid; IR (KBr): 3212, 1697 cm<sup>-1</sup>; <sup>1</sup>H NMR (CDCl<sub>3</sub>): δ 9.78 (br s, 1H), 8.67 (d, 1H, *J* = 8.7 Hz), 8.19 (s, 1H), 8.16 (d, 1H, *J* = 8.4 Hz), 7.71 (m, 1H), 7.59 (m, 1H), 7.16 (m, 1H), 6.68 (m, 2H), 6.57 (m, 1H), 1.88 (m, 15H);

ESIMS: *m/z* 416 (M+1); Anal. Calcd for C<sub>26</sub>H<sub>26</sub>FN<sub>3</sub>O (415.5): C, 75.16; H, 6.31; N, 10.11. Found: C, 75.33; H, 6.10; N, 10.34.

**6.2.5. 4-Adamantan-1-yl-quinoline-2-carboxylic acid *N'*-(4-fluorophenyl)hydrazide (**11**).** Yield: 62%; oil; IR (neat): 3293, 1688 cm<sup>-1</sup>; <sup>1</sup>H NMR (CDCl<sub>3</sub>): 9.76 (br s, 1H), 8.69 (d, 1H, *J* = 8.7 Hz), 8.17 (m, 2H), 7.73 (m, 1H), 7.60 (m, 1H), 6.95 (m, 4H), 6.25 (br s, 1H), 1.88 (m, 15H); APCI MS: *m/z* 416 (M+1); Anal. Calcd for C<sub>26</sub>H<sub>26</sub>FN<sub>3</sub>O (415.5): C, 75.16; H, 6.31; N, 10.11. Found: C, 74.89; H, 6.55; N, 10.23.

## 6.3. General method for the synthesis of 4-adamantan-1-yl-quinoline-2-carboxylic acid *N'*-alkylhydrazides and *N',N'*-dialkylhydrazides (12–27)

To a solution of 4-(adamantan-1-yl)-2-quinolinecarbohydrazide<sup>6</sup> (**2**, 0.3 g, 0.9 mmol) in abs ethyl alcohol (15 mL), aliphatic or aromatic halide (0.27 mmol) was added. Triethylamine (150 μL, 1.08 mmol) was then added to the reaction mixture. Reaction mixture was heated at 80 °C for 8 h. Reaction mixture was cooled to ambient temperature and solvent evaporated under reduced pressure to afford a mixture of mono- and disubstituted hydrazides, which upon chromatographic purification using EtOAc/hexanes (10:90) as eluant gave product.

In the cases involving use of secondary alkyl halides, the above-mentioned procedure proved to be unsuccessful. Alternate experimental procedure described below was used to obtain remaining derivatives.

To a solution of 4-(adamantan-1-yl)-2-quinolinecarbohydrazide<sup>6</sup> (**2**, 0.1 g, 0.3 mmol) in DMF (8 mL), secondary alkyl bromide (0.9 mmol) and K<sub>2</sub>CO<sub>3</sub> (0.1 g, 0.9 mmol) were added. Reaction mixture was stirred at 80 °C for 8 h. Reaction mixture was cooled to ambient temperature, and solvent was evaporated under reduced pressure to provide crude product, which upon chromatographic purification using EtOAc/hexanes (10:90) as eluant produced product.

**6.3.1. 4-Adamantan-1-yl-quinoline-2-carboxylic acid *N'*-propylhydrazide (**12**).** Yield: 38%; semi-solid; IR (KBr): 3274, 1678 cm<sup>-1</sup>; <sup>1</sup>H NMR (CDCl<sub>3</sub>): δ 9.41 (br s, 1H), 8.66 (d, 1H, *J* = 8.8 Hz), 8.25 (s, 1H), 8.12 (d, 1H, *J* = 8.3 Hz), 7.68 (m, 1H), 7.56 (m, 1H), 3.01 (m, 2H), 1.88 (m, 15H), 1.61 (m, 2H), 0.95 (m, 3H); ESIMS: *m/z* 364 (M+1); Anal. Calcd for C<sub>23</sub>H<sub>29</sub>N<sub>3</sub>O (363.5): C, 76.00; H, 8.04; N, 11.56. Found: C, 76.12; H, 8.13; N, 11.63.

**6.3.2. 4-Adamantan-1-yl-quinoline-2-carboxylic acid *N'*,*N'*-dipropylhydrazide (**13**).** Yield: 28%; semi-solid; IR (KBr): 3274, 1678 cm<sup>-1</sup>; <sup>1</sup>H NMR (CDCl<sub>3</sub>): δ 8.66 (d, 1H, *J* = 8.7 Hz), 8.25 (s, 1H), 8.16 (d, 1H, *J* = 8.4 Hz), 7.67 (m, 1H), 7.57 (m, 1H), 2.90 (m, 4H), 1.95 (m, 15H), 1.64 (m, 4H), 0.94 (m, 6H); ESIMS: *m/z* 406 (M+1); Anal. Calcd for C<sub>26</sub>H<sub>35</sub>N<sub>3</sub>O (405.6): C, 77.00; H, 8.70; N, 10.36. Found: C, 77.12; H, 8.81; N, 10.25.

**6.3.3. 4-Adamantan-1-yl-quinoline-2-carboxylic acid *N'*-butylhydrazide (14).** Yield: 45%; semi-solid; IR (KBr): 3268, 1673  $\text{cm}^{-1}$ ;  $^1\text{H}$  NMR ( $\text{CDCl}_3$ ):  $\delta$  8.66 (d, 1H,  $J = 8.6$  Hz), 8.25 (s, 1H), 8.12 (d, 1H,  $J = 9.6$  Hz), 7.68 (m, 1H), 7.56 (m, 1H), 2.98 (m, 2H), 1.87 (m, 15H), 1.58 (m, 4H), 0.89 (m, 3H); ESIMS:  $m/z$  378 (M+1); Anal. Calcd for  $\text{C}_{24}\text{H}_{31}\text{N}_3\text{O}$  (377.5): C, 76.35; H, 8.28; N, 11.13. Found: C, 76.27; H, 8.21; N, 11.07.

**6.3.4. 4-Adamantan-1-yl-quinoline-2-carboxylic acid *N'*, *N'*-dibutylhydrazide (15).** Yield: 30%; semi-solid; IR (KBr): 3274, 1678  $\text{cm}^{-1}$ ;  $^1\text{H}$  NMR ( $\text{CDCl}_3$ ):  $\delta$  8.66 (d, 1H,  $J = 9.2$  Hz), 8.26 (s, 1H), 8.15 (d, 1H,  $J = 8.3$  Hz), 7.69 (m, 1H), 7.56 (m, 1H), 2.87 (m, 4H), 1.88 (m, 15H), 1.58 (m, 4H), 1.33 (m, 4H), 0.88 (m, 6H); ESIMS:  $m/z$  434 (M+1); Anal. Calcd for  $\text{C}_{28}\text{H}_{39}\text{N}_3\text{O}$  (433.6): C, 77.55; H, 9.07; N, 9.69. Found: C, 77.49; H, 9.01; N, 9.75.

**6.3.5. 4-Adamantan-1-yl-quinoline-2-carboxylic acid *N'*-sec-butylhydrazide (16).** Yield: 60%; semi-solid; IR (KBr): 3250, 1685  $\text{cm}^{-1}$ ;  $^1\text{H}$  NMR ( $\text{CDCl}_3$ ):  $\delta$  8.64 (d, 1H,  $J = 8.5$  Hz), 8.35 (d, 1H,  $J = 8.2$  Hz), 8.07 (s, 1H), 7.69 (m, 1H), 7.59 (m, 1H), 3.01 (m, 1H), 1.88 (m, 15H), 1.44 (m, 3H), 1.43 (m, 2H), 1.03 (m, 3H); ESIMS:  $m/z$  378 (M+1); Anal. Calcd for  $\text{C}_{24}\text{H}_{31}\text{N}_3\text{O}$  (377.5): C, 76.35; H, 8.28; N, 11.13. Found: C, 76.21; H, 8.10; N, 11.02.

**6.3.6. 4-Adamantan-1-yl-quinoline-2-carboxylic acid *N'*-hexylhydrazide (17).** Yield: 35%; semi-solid; IR (KBr): 3270, 1673  $\text{cm}^{-1}$ ;  $^1\text{H}$  NMR ( $\text{CDCl}_3$ ):  $\delta$  8.60 (d, 1H,  $J = 8.5$  Hz), 8.27 (s, 1H), 8.10 (d, 1H,  $J = 9.4$  Hz), 7.55 (m, 1H), 7.50 (m, 1H), 2.92 (m, 2H), 1.85 (m, 15H), 1.53 (m, 8H), 0.80 (m, 3H); ESIMS:  $m/z$  406 (M+1); Anal. Calcd for  $\text{C}_{26}\text{H}_{35}\text{N}_3\text{O}$  (405.6): C, 77.00; H, 8.70; N, 10.36. Found: C, 76.74; H, 8.92; N, 10.71.

**6.3.7. 4-Adamantan-1-yl-quinoline-2-carboxylic acid *N'*, *N'*-dihexylhydrazide (18).** Yield: 32%; semi-solid; IR (KBr): 3272, 1675  $\text{cm}^{-1}$ ;  $^1\text{H}$  NMR ( $\text{CDCl}_3$ ):  $\delta$  8.63 (d, 1H,  $J = 9.0$  Hz), 8.30 (s, 1H), 8.20 (d, 1H,  $J = 8.5$  Hz), 7.70 (m, 1H), 7.60 (m, 1H), 2.90 (m, 4H), 1.89 (m, 15H), 1.56 (m, 8H), 1.35 (m, 8H), 0.90 (m, 6H); ESIMS:  $m/z$  488 (M+1); Anal. Calcd for  $\text{C}_{32}\text{H}_{47}\text{N}_3\text{O}$  (487.7): C, 78.48; H, 9.67; N, 8.58. Found: C, 78.21; H, 9.43; N, 8.94.

**6.3.8. 4-Adamantan-1-yl-quinoline-2-carboxylic acid *N'*, *N'*-diallylhydrazide (19).** Yield: 58%; mp: 145–147 °C (dec); IR (KBr): 3252, 1683  $\text{cm}^{-1}$ ;  $^1\text{H}$  NMR ( $\text{CDCl}_3$ ):  $\delta$  8.92 (br s, 1H), 8.64 (d, 1H,  $J = 8.7$  Hz), 8.22 (s, 1H), 8.12 (d, 1H,  $J = 8.3$  Hz), 7.68 (m, 1H), 7.55 (m, 1H), 6.03 (m, 2H), 5.21 (m, 4H), 3.60 (m, 4H), 1.88 (m, 15H); ESIMS:  $m/z$  402 (M+1); Anal. Calcd for  $\text{C}_{26}\text{H}_{31}\text{N}_3\text{O}$  (401.5), calcd: C, 77.77; H, 7.78; N, 10.46. Found: C, 77.58; H, 7.67; N, 10.38.

**6.3.9. 4-Adamantan-1-yl-quinoline-2-carboxylic acid *N'*-cyclopentylhydrazide (20).** Yield: 48%; semi-solid; IR (KBr): 3250, 1700  $\text{cm}^{-1}$ ;  $^1\text{H}$  NMR ( $\text{CDCl}_3$ ):  $\delta$  8.60 (d, 1H,  $J = 8.3$  Hz), 8.33 (d, 1H,  $J = 7.4$  Hz), 8.10 (s, 1H), 7.73 (m, 1H), 7.60 (m, 1H), 2.80 (m, 1H), 1.86 (m,

15H), 1.50 (m, 8H); ESIMS:  $m/z$  390 (M+1); Anal. Calcd for  $\text{C}_{25}\text{H}_{31}\text{N}_3\text{O}$  (389.5): C, 77.08; H, 8.02; N, 10.79. Found: C, 76.87; H, 8.21; N, 10.95.

**6.3.10. 4-Adamantan-1-yl-quinoline-2-carboxylic acid *N'*-cyclohexylhydrazide (21).** Yield: 52%; semi-solid; IR (KBr): 3253, 1707  $\text{cm}^{-1}$ ;  $^1\text{H}$  NMR ( $\text{CDCl}_3$ ):  $\delta$  8.64 (d, 1H,  $J = 8.2$  Hz), 8.35 (d, 1H,  $J = 7.3$  Hz), 8.08 (s, 1H), 7.70 (m, 1H), 7.58 (m, 1H), 2.84 (m, 1H), 1.88 (m, 15H), 1.52 (m, 10H); ESIMS:  $m/z$  404 (M+1); Anal. Calcd for  $\text{C}_{26}\text{H}_{33}\text{N}_3\text{O}$  (403.5): C, 77.38; H, 8.24; N, 10.41. Found: C, 77.56; H, 8.08; N, 10.33.

**6.3.11. 4-Adamantan-1-yl-quinoline-2-carboxylic acid *N'*-isopropylhydrazide (22).** Yield: 54%; semi-solid; IR (KBr): 1706  $\text{cm}^{-1}$ ;  $^1\text{H}$  NMR ( $\text{CDCl}_3$ ):  $\delta$  8.64 (d, 1H,  $J = 8.2$  Hz), 8.34 (d, 1H,  $J = 8.3$  Hz), 8.08 (s, 1H), 7.69 (m, 1H), 7.58 (m, 1H), 3.70 (m, 1H), 1.88 (m, 15H), 1.25 (m, 6H); ESIMS:  $m/z$  364 (M+1); Anal. Calcd for  $\text{C}_{23}\text{H}_{29}\text{N}_3\text{O}$  (363.5): C, 76.00; H, 8.04; N, 11.56. Found: C, 76.11; H, 8.08; N, 11.33.

**6.3.12. 4-Adamantan-1-yl-quinoline-2-carboxylic acid *N'*-phenethylhydrazide (23).** Yield: 36%; semi-solid; IR (KBr): 3250, 1670  $\text{cm}^{-1}$ ;  $^1\text{H}$  NMR ( $\text{CDCl}_3$ ):  $\delta$  8.89 (br s, 1H), 8.67 (d, 1H,  $J = 8.6$  Hz), 8.28 (s, 1H), 8.17 (d, 1H,  $J = 8.3$  Hz), 7.71 (m, 1H), 7.59 (m, 1H), 7.26 (m, 5H), 3.21 (m, 2H), 2.94 (m, 2H), 1.88 (m, 15H); ESIMS:  $m/z$  426 (M+1); Anal. Calcd for  $\text{C}_{28}\text{H}_{31}\text{N}_3\text{O}$  (425.6): C, 79.02; H, 7.34; N, 9.87. Found: C, 79.11; H, 7.45; N, 9.93.

**6.3.13. 4-Adamantan-1-yl-quinoline-2-carboxylic acid *N'*, *N'*-diphenethylhydrazide (24).** Yield: 25%; mp: 180–181 °C (dec); IR (KBr): 3276, 1688  $\text{cm}^{-1}$ ;  $^1\text{H}$  NMR ( $\text{CDCl}_3$ ):  $\delta$  9.43 (br s, 1H), 8.65 (d, 1H,  $J = 8.6$  Hz), 8.19 (s, 1H), 8.11 (d, 1H,  $J = 8.3$  Hz), 7.68 (m, 1H), 7.56 (m, 1H), 7.30 (m, 10H), 3.30 (m, 4H), 2.93 (m, 4H), 1.88 (m, 15H); ESIMS:  $m/z$  530 (M+1); Anal. Calcd for  $\text{C}_{36}\text{H}_{39}\text{N}_3\text{O}$  (529.7): C, 81.63; H, 7.42; N, 7.93. Found: C, 81.75; H, 7.35; N, 7.85.

**6.3.14. 4-Adamantan-1-yl-quinoline-2-carboxylic acid *N'*-(3-phenylpropyl)hydrazide (25).** Yield: 36%; semi-solid; IR (KBr): 3240, 1670  $\text{cm}^{-1}$ ;  $^1\text{H}$  NMR ( $\text{CDCl}_3$ ):  $\delta$  8.85 (br s, 1H), 8.65 (d, 1H,  $J = 8.5$  Hz), 8.30 (s, 1H), 8.20 (d, 1H,  $J = 8.4$  Hz), 7.70 (m, 1H), 7.60 (m, 1H), 7.24 (m, 5H), 3.22 (m, 2H), 2.90 (m, 2H), 2.07 (m, 2H), 1.87 (m, 15H); ESIMS:  $m/z$  440 (M+1); Anal. Calcd for  $\text{C}_{29}\text{H}_{33}\text{N}_3\text{O}$  (439.6): C, 79.23; H, 7.57; N, 9.56. Found: C, 79.46; H, 7.65; N, 9.44.

**6.3.15. 4-Adamantan-1-yl-quinoline-2-carboxylic acid *N'*, *N'*-bis-(3-phenylpropyl)hydrazide (26).** Yield: 23%; mp: 171–173 °C (dec); IR (KBr): 3270, 1685  $\text{cm}^{-1}$ ;  $^1\text{H}$  NMR ( $\text{CDCl}_3$ ):  $\delta$  9.40 (br s, 1H), 8.63 (d, 1H,  $J = 8.5$  Hz), 8.21 (s, 1H), 8.09 (d, 1H,  $J = 8.5$  Hz), 7.70 (m, 1H), 7.60 (m, 1H), 7.28 (m, 10H), 3.31 (m, 4H), 2.91 (m, 4H), 2.10 (m, 4H), 1.88 (m, 15H); ESIMS:  $m/z$  578 (M+1); Anal. Calcd for  $\text{C}_{38}\text{H}_{43}\text{N}_3\text{O}$  (577.8): C, 81.83; H, 7.77; N, 7.53. Found: C, 81.65; H, 7.50; N, 7.91.



**6.3.16. Benzoic acid *N'*-(4-adamantan-1-yl-quinoline-2-carbonyl)-*N*-benzoylhydrazide (27).** Yield: 45%; mp: 144–146 °C (dec); IR (KBr): 3260, 1680, 1630 cm<sup>-1</sup>; <sup>1</sup>H NMR (CDCl<sub>3</sub>): δ 9.21 (br s, 1H), 8.60 (d, 1H, *J* = 8.5 Hz), 8.23 (s, 1H), 8.10 (d, 1H, *J* = 8.5 Hz), 8.01 (m, 2H), 7.72 (m, 1H), 7.63 (m, 1H), 7.50 (m, 3H), 1.88 (m, 15H); ESIMS: *m/z* 426 (M+1); Anal. Calcd for C<sub>27</sub>H<sub>27</sub>N<sub>3</sub>O (425.5): C, 76.21; H, 6.40; N, 9.87. Found: C, 76.03; H, 6.55; N, 9.74.

**6.4. General method for the synthesis of 4-adamantan-1-yl-quinoline-2-carboxylic acid alkylidene hydrazides (28–49)**

To a solution of 4-(adamantan-1-yl)-2-quinolinecarboxylic acid alkylidene hydrazide<sup>6</sup> (**2**, 0.4 g, 1.2 mmol) in abs ethyl alcohol (20 mL), aliphatic, aromatic or heteroaromatic aldehyde (1.44 mmol) was added, and the reaction mixture was heated at 80 °C for 2 h. The solvent was removed under reduced pressure, and resulting residue was diluted with ethyl acetate (50 mL). Organic layer was washed with water (2 × 15 mL) followed by brine (15 mL), and dried (Na<sub>2</sub>SO<sub>4</sub>). The solvent was removed under reduced pressure to afford crude product, which upon chromatographic purification over neutral alumina using EtOAc/hexanes (5:95) produced 4-adamantan-1-yl-quinoline-2-carboxylic acid alkylidene hydrazides **28–49**.

**6.4.1. 4-Adamantan-1-yl-quinoline-2-carboxylic acid propylidenehydrazide (28).** Yield: 55%; mp: 147–148 °C; IR (KBr): 3436, 1676 cm<sup>-1</sup>; <sup>1</sup>H NMR (CDCl<sub>3</sub>): 10.90 (br s, 1H), 8.68 (d, 1H, *J* = 8.80 Hz), 8.30 (s, 1H), 8.14 (d, 1H, *J* = 8.40 Hz), 7.72 (m, 2H), 7.58 (m, 1H), 2.48 (m, 2H), 1.89 (m, 15H), 1.20 (t, 3H, *J* = 7.50 Hz); APCIMS: *m/z* 362 (M+1); Anal. Calcd for C<sub>23</sub>H<sub>27</sub>N<sub>3</sub>O (361.5): C, 76.42; H, 7.53; N, 11.62. Found: C, 76.64; H, 7.80; N, 11.45.

**6.4.2. 4-Adamantan-1-yl-quinoline-2-carboxylic acid isobutylidenehydrazide (29).** Yield: 48%; mp: 213–215 °C; IR (KBr): 3306, 1688 cm<sup>-1</sup>; <sup>1</sup>H NMR (CDCl<sub>3</sub>): 10.83 (br s, 1H), 8.68 (d, 1H, *J* = 8.7 Hz), 8.30 (s, 1H), 8.13 (d, 1H, *J* = 8.3 Hz), 7.70 (m, 1H), 7.58 (m, 2H), 2.78 (m, 1H), 1.89 (m, 15H), 1.19 (d, 6H, *J* = 6.7 Hz); APCIMS: *m/z* 376 (M+1); Anal. Calcd for C<sub>24</sub>H<sub>29</sub>N<sub>3</sub>O (375.5): C, 76.76; H, 7.78; N, 11.19. Found: C, 76.93; H, 7.65; N, 11.11.

**6.4.3. 4-Adamantan-1-yl-quinoline-2-carboxylic acid (2,2-dimethylpropylidene)hydrazide (30).** Yield: 66%; mp: 140–142 °C (dec); IR (KBr): 3309, 1686 cm<sup>-1</sup>; <sup>1</sup>H NMR (CDCl<sub>3</sub>): δ 10.79 (br s, 1H), 8.67 (d, 1H, *J* = 8.6 Hz), 8.29 (s, 1H), 8.13 (d, 1H, *J* = 8.8 Hz), 7.70 (m, 2H), 7.59 (m, 1H), 1.88 (m, 15H), 1.23 (m, 9H); ESIMS: *m/z* 391 (M+1); Anal. Calcd for C<sub>25</sub>H<sub>31</sub>N<sub>3</sub>O (389.5): C, 77.08; H, 8.02; N, 10.79. Found: C, 77.41; H, 7.84; N, 11.03.

**6.4.4. 4-Adamantan-1-yl-quinoline-2-carboxylic acid benzylidenehydrazide (31).** Yield: 66%; mp: 184–186 °C; IR (KBr): 3280, 1675 cm<sup>-1</sup>; <sup>1</sup>H NMR (CDCl<sub>3</sub>): δ 11.09 (br s, 1H), 8.80 (d, 1H, *J* = 8.4 Hz), 8.40 (s, 1H), 8.31 (s, 1H), 8.07 (d, 1H, *J* = 8.4 Hz), 7.85 (m, 2H), 7.65

(m, 5H), 1.89 (m, 15H); APCIMS: *m/z* 410 (M+1); Anal. Calcd for C<sub>27</sub>H<sub>27</sub>N<sub>3</sub>O (409.5): C, 79.19; H, 6.65; N, 10.26. Found: C, 78.87; H, 6.75; N, 10.45.

**6.4.5. 4-Adamantan-1-yl-quinoline-2-carboxylic acid (3-hydroxybenzylidene)hydrazide (32).** Yield: 66%; mp: 193–195 °C; IR (KBr): 3275, 1677 cm<sup>-1</sup>; <sup>1</sup>H NMR (CDCl<sub>3</sub>): δ 11.21 (br s, 1H), 8.75 (d, 1H, *J* = 8.3 Hz), 8.36 (s, 1H), 8.28 (s, 1H), 8.03 (d, 1H, *J* = 8.2 Hz), 7.85 (m, 1H), 7.71 (m, 2H), 7.65 (m, 2H), 7.50 (m, 1H), 1.89 (m, 15H); APCIMS: *m/z* 426 (M+1); Anal. Calcd for C<sub>27</sub>H<sub>27</sub>N<sub>3</sub>O<sub>2</sub> (425.5): C, 76.21; H, 6.40; N, 9.87. Found: C, 76.29; H, 6.31; N, 9.95.

**6.4.6. 4-Adamantan-1-yl-quinoline-2-carboxylic acid (4-hydroxybenzylidene)hydrazide (33).** Yield: 66%; mp: 201–203 °C; IR (KBr): 3275, 1680 cm<sup>-1</sup>; <sup>1</sup>H NMR (CDCl<sub>3</sub>): δ 11.18 (br s, 1H), 8.71 (d, 1H, *J* = 8.7 Hz), 8.40 (s, 1H), 8.30 (s, 1H), 8.08 (d, 1H, *J* = 8.3 Hz), 7.85 (d, 2H, *J* = 8.5 Hz), 7.70 (m, 1H), 7.55 (m, 1H), 6.91 (d, 2H, *J* = 8.5 Hz), 1.88 (m, 15H); APCIMS: *m/z* 426 (M+1); Anal. Calcd for C<sub>27</sub>H<sub>27</sub>N<sub>3</sub>O<sub>2</sub> (425.5): C, 76.21; H, 6.40; N, 9.87. Found: C, 76.03; H, 6.57; N, 9.51.

**6.4.7. 4-Adamantan-1-yl-quinoline-2-carboxylic acid (4-methoxybenzylidene)hydrazide (34).** Yield: 71%; mp: >250 °C; IR (KBr): 3268, 1685 cm<sup>-1</sup>; <sup>1</sup>H NMR (CDCl<sub>3</sub>): δ 11.12 (br s, 1H), 8.69 (d, 1H, *J* = 8.80 Hz), 8.36 (s, 1H), 8.33 (s, 1H), 8.16 (d, 1H, *J* = 8.2 Hz), 7.80 (d, 2H, *J* = 8.6 Hz), 7.72 (m, 1H), 7.59 (m, 1H), 6.95 (d, 2H, *J* = 8.7 Hz), 3.86 (s, 3H), 1.90 (m, 15H); APCIMS: *m/z* 440 (M+1); Anal. Calcd for C<sub>28</sub>H<sub>29</sub>N<sub>3</sub>O<sub>2</sub> (439.6): C, 76.51; H, 6.65; N, 9.56. Found: C, 76.86; H, 6.37; N, 9.48.

**6.4.8. 4-Adamantan-1-yl-quinoline-2-carboxylic acid (2-chlorobenzylidene)hydrazide (35).** Yield: 67%; mp: 142–144 °C; IR (KBr): 3270, 1680 cm<sup>-1</sup>; <sup>1</sup>H NMR (CDCl<sub>3</sub>): δ 11.10 (br s, 1H), 8.70 (d, 1H, *J* = 8.4 Hz), 8.38 (s, 1H), 8.29 (s, 1H), 8.20 (d, 1H, *J* = 8.4 Hz), 7.75 (m, 1H), 7.61 (m, 1H), 7.40 (m, 4H), 1.90 (m, 15H); APCIMS: *m/z* 444 (M+1); Anal. Calcd for C<sub>27</sub>H<sub>26</sub>ClN<sub>3</sub>O (443.9): C, 73.04; H, 5.90; N, 9.46. Found: C, 72.85; H, 5.95; N, 9.21.

**6.4.9. 4-Adamantan-1-yl-quinoline-2-carboxylic acid pentafluorophenylmethylenhydrazide (36).** Yield: 64%; mp: 225–227 °C; IR (KBr): 2913, 1700 cm<sup>-1</sup>; <sup>1</sup>H NMR (CDCl<sub>3</sub>): δ 11.46 (br s, 1H), 8.73 (m, 2H), 8.31 (s, 1H), 8.18 (d, 1H, *J* = 8.2 Hz), 7.74 (m, 1H), 7.62 (m, 1H), 1.90 (m, 15H); ESIMS: *m/z* 500 (M+1); Anal. Calcd for C<sub>27</sub>H<sub>22</sub>F<sub>5</sub>N<sub>3</sub>O (499.5): C, 64.93; H, 4.44; N, 8.41. Found: C, 65.24; H, 4.62; N, 8.45.

**6.4.10. 4-Adamantan-1-yl-quinoline-2-carboxylic acid (3,5-bis-trifluoromethyl-benzylidene)hydrazide (37).** Yield: 58%; mp: 138–140 °C (dec); IR (KBr): 3223, 1688 cm<sup>-1</sup>; <sup>1</sup>H NMR (CDCl<sub>3</sub>): δ 11.42 (br s, 1H), 8.72 (d, 1H, *J* = 8.6 Hz), 8.64 (s, 1H), 8.31 (m, 3H), 8.18 (d, 1H, *J* = 8.2 Hz), 7.91 (s, 1H), 7.75 (m, 1H), 7.63 (m, 1H), 1.88 (m, 15H); ESIMS: *m/z* 546 (M+1); Anal. Calcd for C<sub>29</sub>H<sub>25</sub>F<sub>6</sub>N<sub>3</sub>O (545.2): C, 63.85; H, 4.62; N, 7.70. Found: C, 63.93; H, 4.54; N, 7.85.

**6.4.11. 4-Adamantan-1-yl-quinoline-2-carboxylic acid (2-methoxynaphthalen-1-ylmethylene)hydrazide (38).** Yield: 43%; mp: 138–140 °C (dec); IR (KBr): 3216, 1685 cm<sup>-1</sup>; <sup>1</sup>H NMR (CDCl<sub>3</sub>): δ 11.23 (br s, 1H), 8.98 (s, 1H), 8.87 (d, 1H, *J* = 8.5 Hz), 8.71 (d, 1H, *J* = 8.6 Hz), 8.35 (m, 2H), 8.24 (m, 1H), 8.06 (d, 1H, *J* = 8.2 Hz), 7.65 (m, 4H), 6.90 (d, 1H, *J* = 8.2 Hz), 4.07 (s, 3H), 1.88 (m, 15H); ESIMS: *m/z* 490 (M+1); Anal. Calcd for C<sub>32</sub>H<sub>31</sub>N<sub>3</sub>O<sub>2</sub> (489.6): C, 78.50; H, 6.38; N, 8.58. Found: C, 78.75; H, 6.63; N, 8.85.

**6.4.12. 4-Adamantan-1-yl-quinoline-2-carboxylic acid (4-methoxynaphthalen-1-ylmethylene)hydrazide (39).** Yield: 55%; mp: 162–164 °C (dec); IR (KBr): 3436, 1790 cm<sup>-1</sup>; <sup>1</sup>H NMR (CDCl<sub>3</sub>): δ 11.23 (br s, 1H), 8.99 (s, 1H), 8.87 (d, 1H, *J* = 8.9 Hz), 8.71 (d, 1H, *J* = 8.6 Hz), 8.35 (m, 2H), 8.22 (d, 1H, *J* = 8.3 Hz), 8.06 (d, 1H, *J* = 8.3 Hz), 7.64 (m, 4H), 6.91 (d, 1H, *J* = 8.2 Hz), 4.11 (s, 3H), 1.88 (m, 15H); ESIMS: *m/z* 490 (M+1); Anal. Calcd for C<sub>32</sub>H<sub>31</sub>N<sub>3</sub>O<sub>2</sub> (489.6): C, 78.50; H, 6.38; N, 8.58. Found: C, 78.65; H, 6.41; N, 8.36.

**6.4.13. 4-Adamantan-1-yl-quinoline-2-carboxylic acid (4-dimethylaminonaphthalen-1-ylmethylene)hydrazide (40).** Yield: 61%; mp: 152–154 °C (dec); IR (KBr): 3244, 1651 cm<sup>-1</sup>; <sup>1</sup>H NMR (CDCl<sub>3</sub>): δ 11.24 (br s, 1H), 9.00 (s, 1H), 8.87 (d, 1H, *J* = 8.3 Hz), 8.71 (d, 1H, *J* = 8.8 Hz), 8.37 (s, 1H), 8.25 (m, 2H), 8.03 (d, 1H, *J* = 7.9 Hz), 7.74 (m, 1H), 7.58 (m, 3H), 7.90 (d, 1H, *J* = 7.9 Hz), 2.99 (s, 6H), 1.88 (m, 15H); ESIMS: *m/z* 503 (M+1); Anal. Calcd for C<sub>33</sub>H<sub>34</sub>N<sub>4</sub>O (502.6): C, 78.85; H, 6.82; N, 11.15. Found: C, 78.91; H, 6.92; N, 11.37.

**6.4.14. 4-Adamantan-1-yl-quinoline-2-carboxylic acid anthracen-9-ylmethylenehydrazide (41).** Yield: 50%; mp: 158–160 °C (dec); IR (KBr): 3232, 1688 cm<sup>-1</sup>; <sup>1</sup>H NMR (CDCl<sub>3</sub>): δ 11.55 (br s, 1H), 9.67 (s, 1H), 8.74 (m, 3H), 8.54 (s, 1H), 8.42 (s, 1H), 8.27 (d, 1H, *J* = 9.6 Hz), 8.05 (d, 2H, *J* = 8.3 Hz), 7.77 (m, 1H), 7.57 (m, 5H), 1.88 (m, 15H); ESIMS: *m/z* 510 (M+1); Anal. Calcd for C<sub>35</sub>H<sub>31</sub>N<sub>3</sub>O (509.6): C, 82.48; H, 6.13; N, 8.25. Found: C, 82.47; H, 6.08; N, 8.21.

**6.4.15. 4-Adamantan-1-yl-quinoline-2-carboxylic acid (1H-pyrrol-2-ylmethylene)hydrazide (42).** Yield: 66%; mp: 130–132 °C (dec); IR (KBr): 3296, 1693 cm<sup>-1</sup>; <sup>1</sup>H NMR (CDCl<sub>3</sub>): δ 11.03 (br s, 1H), 9.95 (br s, 1H), 8.69 (d, 1H, *J* = 8.7 Hz), 8.30 (s, 1H), 8.16 (m, 2H), 7.72 (m, 1H), 7.59 (m, 1H), 6.98 (d, 1H, *J* = 4.4 Hz), 6.54 (d, 1H, *J* = 4.2 Hz), 6.27 (m, 1H), 1.88 (m, 15H); ESIMS: *m/z* 399 (M+1); Anal. Calcd for C<sub>25</sub>H<sub>26</sub>N<sub>4</sub>O (398.5): C, 75.35; H, 6.58; N, 14.06. Found: C, 75.51; H, 6.35; N, 14.41.

**6.4.16. 4-Adamantan-1-yl-quinoline-2-carboxylic acid thiophen-2-ylmethylenehydrazide (43).** Yield: 60%; mp: 138–140 °C (dec); IR (KBr): 3291, 1682 cm<sup>-1</sup>; <sup>1</sup>H NMR (DMSO-*d*<sub>6</sub>): δ 12.19 (br s, 1H), 8.92 (s, 1H), 8.78 (d, 1H, *J* = 8.4 Hz), 8.26 (d, 1H, *J* = 8.1 Hz), 8.10 (s, 1H), 7.87 (m, 1H), 7.75 (m, 2H), 7.50 (d, 1H, *J* = 3.2 Hz), 7.19 (m, 1H), 1.88 (m, 15H); ESIMS: *m/z* 416 (M+1); Anal. Calcd for C<sub>25</sub>H<sub>25</sub>N<sub>3</sub>OS (415.6): C,

72.26; H, 6.06; N, 10.11. Found: C, 72.35; H, 6.13; N, 10.18.

**6.4.17. 4-Adamantan-1-yl-quinoline-2-carboxylic acid furan-2-ylmethylenehydrazide (44).** Yield: 50%; mp: 135–138 °C (dec); IR (KBr): 3298, 1701 cm<sup>-1</sup>; <sup>1</sup>H NMR (CDCl<sub>3</sub>): δ 11.17 (br s, 1H), 8.69 (d, 1H, *J* = 8.6 Hz), 8.50 (s, 1H), 8.31 (s, 1H), 8.15 (d, 1H, *J* = 8.1 Hz), 7.60 (m, 2H), 7.48 (m, 1H), 6.90 (d, 1H, *J* = 4.2 Hz), 6.52 (d, 1H, *J* = 4.1 Hz), 1.88 (m, 15H); ESIMS: *m/z* 400 (M+1); Anal. Calcd for C<sub>25</sub>H<sub>25</sub>N<sub>3</sub>O<sub>2</sub> (399.5): C, 75.16; H, 6.31; N, 10.52. Found: C, 74.19; H, 6.37; N, 10.55.

**6.4.18. 4-Adamantan-1-yl-quinoline-2-carboxylic acid pyridin-2-ylmethylenehydrazide (45).** Yield: 60%; mp: 140–142 °C (dec); IR (KBr): 3293, 1712 cm<sup>-1</sup>; <sup>1</sup>H NMR (CDCl<sub>3</sub>): δ 11.37 (br s, 1H), 8.68 (m, 2H), 8.44 (s, 1H), 8.33 (s, 1H), 8.29 (d, 1H, *J* = 8.0 Hz), 8.20 (d, 1H, *J* = 7.9 Hz), 7.75 (m, 2H), 7.61 (m, 1H), 7.31 (m, 1H), 1.88 (m, 15H); ESIMS: *m/z* 411 (M+1); Anal. Calcd for C<sub>26</sub>H<sub>26</sub>N<sub>4</sub>O (410.5): C, 76.07; H, 6.38; N, 13.65. Found: C, 75.81; H, 6.39; N, 13.52.

**6.4.19. 4-Adamantan-1-yl-quinoline-2-carboxylic acid pyridin-3-ylmethylenehydrazide (46).** Yield: 61%; mp: 130–132 °C (dec); IR (KBr): 3298, 1709 cm<sup>-1</sup>; <sup>1</sup>H NMR (DMSO-*d*<sub>6</sub>): δ 12.35 (br s, 1H), 8.88 (s, 1H), 8.77 (m, 2H), 8.64 (d, 1H, *J* = 3.9 Hz), 8.27 (d, 1H, *J* = 8.2 Hz), 8.19 (d, 1H, *J* = 8.1 Hz), 8.11 (s, 1H), 7.87 (m, 1H), 7.75 (m, 1H), 7.53 (m, 1H), 1.88 (m, 15H); ESIMS: *m/z* 411 (M+1); Anal. Calcd for C<sub>26</sub>H<sub>26</sub>N<sub>4</sub>O (410.5): C, 76.07; H, 6.38; N, 13.65. Found: C, 76.12; H, 6.41; N, 13.62.

**6.4.20. 4-Adamantan-1-yl-quinoline-2-carboxylic acid pyridin-4-ylmethylenehydrazide (47).** Yield: 62%; mp: 138–140 °C (dec); IR (KBr): 3293, 1714 cm<sup>-1</sup>; <sup>1</sup>H NMR (CDCl<sub>3</sub>): δ 11.41 (br s, 1H), 8.71 (m, 3H), 8.48 (s, 1H), 8.32 (s, 1H), 8.17 (d, 1H, *J* = 7.9 Hz), 7.73 (m, 3H), 7.62 (m, 1H), 1.88 (m, 15H); ESIMS: *m/z* 411 (M+1); Anal. Calcd for C<sub>26</sub>H<sub>26</sub>N<sub>4</sub>O (410.5): C, 76.07; H, 6.38; N, 13.65. Found: C, 76.15; H, 6.44; N, 13.47.

**6.4.21. 4-Adamantan-1-yl-quinoline-2-carboxylic acid quinolin-4-ylmethylenehydrazide (48).** Yield: 53%; mp: 142–144 °C (dec); IR (KBr): 3245, 1683 cm<sup>-1</sup>; <sup>1</sup>H NMR (CDCl<sub>3</sub>): δ 11.53 (br s, 1H), 9.21 (m, 1H), 9.01 (d, 1H, *J* = 4.4 Hz), 8.71 (m, 2H), 8.30 (s, 1H), 8.21 (m, 2H), 7.98 (d, 1H, *J* = 4.5 Hz), 7.71 (m, 4H), 1.88 (m, 15H); ESIMS: *m/z* 461 (M+1); Anal. Calcd for C<sub>30</sub>H<sub>28</sub>N<sub>4</sub>O (460.5): C, 78.23; H, 6.13; N, 12.16. Found: C, 78.04; H, 6.27; N, 12.43.

**6.4.22. 4-Adamantan-1-yl-quinoline-2-carboxylic acid (7-chloroquinolin-4-ylmethylene)hydrazide (49).** Yield: 55%; mp: 127–129 °C (dec); IR (KBr): 3250, 1685 cm<sup>-1</sup>; <sup>1</sup>H NMR (CDCl<sub>3</sub>): δ 11.44 (br s, 1H), 9.30 (m, 1H), 8.95 (d, 1H, *J* = 4.3 Hz), 8.71 (m, 2H), 8.35 (s, 1H), 8.25 (m, 2H), 7.89 (d, 1H, *J* = 4.4 Hz), 7.75 (m, 3H), 1.89 (m, 15H); ESIMS: *m/z* 496 (M+1); Anal. Calcd for C<sub>30</sub>H<sub>27</sub>ClN<sub>4</sub>O (495.0): C, 72.79; H, 5.50; N, 11.32. Found: C, 72.58; H, 5.31; N, 11.49.



### Acknowledgments

The authors are thankful to the Tuberculosis Antimicrobial Acquisition and Coordination Facility (TAACF), which provided partial antimycobacterial data through a research and development contract with the U.S. National Institute of Allergy and Infectious Diseases. Amit Nayyar and Alpeshkumar Malde thank the Council of Scientific and Industrial Research (CSIR), India, for the award of a Senior Research Fellowship. The computational facilities at BCP were provided by the Department of Science and Technology (DST), India, through a grant (SR/FST/LS1–083/2003) under the FIST program.

### References and notes

- World Health Organization, Tuberculosis Fact Sheet, No. 104, 2006; please see: [www.who.int/mediacentre/factsheets/fs104/en/](http://www.who.int/mediacentre/factsheets/fs104/en/).
- Nayyar, A.; Jain, R. *Curr. Med. Chem.* **2005**, *12*, 1873.
- Jain, R.; Vaitilingam, B.; Nayyar, A.; Palde, P. B. *Bioorg. Med. Chem. Lett.* **2003**, *13*, 1051.
- Vangapandu, S.; Jain, M.; Jain, R.; Kaur, S.; Singh, P. P. *Bioorg. Med. Chem.* **2004**, *12*, 2501.
- Vaitilingam, B.; Nayyar, A.; Palde, P. B.; Monga, V.; Jain, R.; Kaur, S.; Singh, P. P. *Bioorg. Med. Chem.* **2004**, *12*, 4179.
- Monga, V.; Nayyar, A.; Vaitilingam, B.; Palde, P. B.; Jhamb, S. S.; Kaur, S.; Singh, P. P.; Jain, R. *Bioorg. Med. Chem.* **2004**, *12*, 6465.
- Nayyar, A.; Malde, A.; Jain, R.; Coutinho, E. *Bioorg. Med. Chem.* **2006**, *14*, 847.
- Nayyar, A.; Malde, A.; Coutinho, E.; Jain, R. *Bioorg. Med. Chem.* **2006**, *14*, 7302.
- Minisci, F.; Bernardi, R.; Berlin, F.; Galli, R.; Perchinnunmo, M. A. *Tetrahedron* **1971**, *27*, 3575.
- Minisci, F.; Vismara, E.; Fontana, F. *Heterocycles* **1989**, *28*, 489.
- Franzblau, S. G.; Witzig, R. S.; McLaughlin, J. C.; Torres, P.; Madico, G.; Hernandez, A.; Degnan, M. T.; Cook, M. B.; Quenzer, V. K.; Ferguson, R. M.; Gilman, R. H. *J. Clin. Microbiol.* **1998**, *36*, 362.
- Collins, L.; Franzblau, S. G. *Antimicrob. Agents Chemother.* **1997**, *41*, 1004.
- Martin, E. J.; Blaney, J. M.; Siani, M. A.; Spellmeyer, D. C.; Wong, A. K.; Moos, W. H. *J. Med. Chem.* **1995**, *39*, 1431.
- CoMFA and QSAR Manual, Sybyl 7.1, Associates Inc., 1699 S Hanley Rd., St. Louis, MO 63144, USA.
- Cramer, R. D.; Patterson, D. E.; Bunce, J. D. *J. Am. Chem. Soc.* **1988**, *110*, 5959.
- Klebe, G.; Abraham, U.; Mietzner, T. *J. Med. Chem.* **1994**, *37*, 4130.
- Kellogg, G. E.; Semus, S. F.; Abraham, D. J. *J. Comput.-Aid. Mol. Des.* **1991**, *5*, 545–552.
- Sybyl 7.1, Tripos Associates Inc., 1699 S Hanley Rd., St. Louis, MO 63144, USA.
- (a) Ming-Li, L.; Jian-Min, D.; Da-Cheng, L.; Da-Qi, W. *Acta Cryst.* **2006**, *E62*, o1009–o1010; (b) Muir, K. W.; Morris, D. G. *Acta Cryst.* **2003**, *E59*, o490–o492; (c) Cui-Cui, Y.; Li, W.; Zhi-Yong, X.; Xue-Fang, S. *Acta Cryst.* **2006**, *E62*, o3274–o3275.
- Halgren, T. A. *J. Am. Chem. Soc.* **1990**, *112*, 4710.
- Bush, B. L.; Nachbar, R. B. *J. Comput.-Aid. Mol. Des.* **1993**, *7*, 587.
- Cramer, R. D., III; Bunce, J. D.; Patterson, D. E.; Frank, I. E. *Quant. Struct.-Act. Relat.* **1988**, *7*, 18.
- Clark, M.; Cramer, R. D.; Jones, D. M.; Patterson, D. E.; Simeroth, P. E. *Tetrahedron Comput. Methodol.* **1990**, *3*, 47.